Monte Carlo Study of Transport Properties of InN

S. Vitanov and V. Palankovski

Advanced Material and Device Analysis Group, IuE, TU Vienna, Austria

Abstract. We use a Monte Carlo approach to investigate the electron transport in Indium Nitride. Simulations with two different setups (one with a bandgap of 1.89 eV and one with bandgap of 0.69 eV) are conducted. All relevant scattering mechanisms are accounted for. Results for electron mobility as a function of free carrier concentration and electric field are compared to previous studies and discussed.

1 Introduction and Monte Carlo Setup

In recent years Indium Nitride (InN) has attracted much attention due to the considerable advancement in the growth of high quality crystals. Furthermore, several new works on the material properties proposed a bandgap of ≈0.7 eV [1, 2, 3], instead of ≈1.9 eV [4]. In this work we use a Monte Carlo (MC) approach to investigate the electron transport, considering two band structures [5, 6]. Our calculations include the three lowest valleys of the conduction band (depending on the chosen band structure, see Table 1) and account for non-parabolicity effects. Several stochastic mechanisms such as acoustic phonon, polar optical phonon, inter-valley phonon, Coulomb, and piezoelectric scattering are considered and their impact is assessed. The parameter values for the acoustic deformation potential (ADP Ξ=7.1 eV), polar-optical phonon scattering ($\hbar\omega_{LO}$=73 meV or 89 meV), inter-valley scattering ($\hbar\omega_{iv}=\hbar\omega_{LO}$), mass density ($\rho$=6.81 g/cm^3), and static and high-frequency dielectric constants (ε_s=15.3 and ε_∞=8.4) are adopted from [7, 8]. In addition, we study the influence of another set of dielectric constants (ε_s=11.0 and ε_∞=6.7) recently proposed in [9] in conjunction with the narrow bandgap and lower effective mass.

An accurate piezoelectric scattering model, which accounts for non-parabolicity and wurtzite crystal structure is also employed [10]. Table 2 summarizes experimental values for the elastic constants (c_{11}, c_{12}, and c_{44}) of wurtzite InN. From them we calculate the corresponding longitudinal and transversal elastic constants (c_L and c_T) and sound velocities (v_{sl} and v_{st}). Table 3 gives theoretical values of the piezo-coefficients e_{31} and e_{33} available in the literature and the calculated corresponding $\langle e^2_L \rangle$ and $\langle e^2_T \rangle$ ($e_{15}=e_{31}$ is assumed). Choosing the set of elastic constants from [11] and piezo coefficients from [12] results in a piezo-coupling coefficient K_{av}=0.24.

Table 1. Summary of material parameters of wurtzite InN for MC simulation.

Bandgap Energy			Electron Mass			Non-parabolicity			Scattering models			Ref.
Γ_1 [eV]	A [eV]	Γ_3 [eV]	$m_{\Gamma 1}$ [m_0]	m_A [m_0]	$m_{\Gamma 3}$ [m_0]	$\alpha_{\Gamma 1}$ [1/eV]	α_A [1/eV]	$\alpha_{\Gamma 3}$ [1/eV]	$\hbar\omega_{LO}$ [meV]	ε_s [-]	ε_∞ [-]	
1.89	4.09	4.49	0.11	0.4	0.6	0.419	0.088	0.036	-	-	-	[5]
1.89	-	-	0.11	-	-	-	-	-	89	15.3	8.4	[7]
1.89	4.09	4.49	0.11	0.4	0.6	0.419	0.088	0.036	89	15.3	8.4	[13]
1.86	-	-	0.11	-	-	0.419	-	-	89	15.3	8.4	[14]
1.89	**4.09**	**4.49**	**0.11**	**0.4**	**0.6**	**0.419**	**0.088**	**0.036**	**89**	**15.3**	**8.4**	

Γ_1 [eV]	Γ_3 [eV]	M-L [eV]	$m_{\Gamma 1}$ [m_0]	$m_{\Gamma 3}$ [m_0]	m_{ML} [m_0]	$\alpha_{\Gamma 1}$ [1/eV]	$\alpha_{\Gamma 3}$ [1/eV]	$\alpha_{M\text{-}L}$ [1/eV]	$\hbar\omega_{LO}$ [meV]	ε_s [-]	ε_∞ [-]	
0.69	2.47	3.39	0.04	0.25	1	1.413	0	0	73	15.3	8.4	[8]
0.69	**2.47**	**3.39**	**0.04**	**0.25**	**1**	**1.413**	**0**	**0**	**73/89**	**11.0**	**6.7**	

Table 2. Summary of elastic constants of InN and the resulting longitudinal and transverse elastic constants and sound velocities.

c_{11} [GPa]	c_{12} [GPa]	c_{44} [GPa]	c_L [GPa]	c_T [GPa]	v_{sl} [m/s]	v_{st} [m/s]	Ref.
-	-	-	265	44	6240	2550	[7]
223	115	48	218	50	5660	2720	[11]
190	104	10	163	23	4901	1845	[15]
271	124	46	248	57	6046	2893	[16]
258	113	53	242	61	5966	2987	[17]

Table 3. Summary of piezo coefficients of InN for MC simulation of piezo scattering.

e_{31} [C/m^2]	e_{33} [C/m^2]	$\langle e_L^2 \rangle$ [C^2/m^4]	$\langle e_T^2 \rangle$ [C^2/m^4]	Ref.
-0.57	0.97	0.17	0.72	[12]
-0.11	0.81–1.09	0.13	0.16–0.58	[18]

2 Simulation Results and Discussion

Simulations with two different setups were conducted: one with bandgap of 1.89 eV (effective mass $0.11m_0$ in the Γ_1 valley [5]), and one with bandgap of 0.69 eV (effective mass of $0.04m_0$ [6]), as summarized in Table 1. Results for electron mobility as a function of lattice temperature, free carrier concentration, and electric field were obtained.

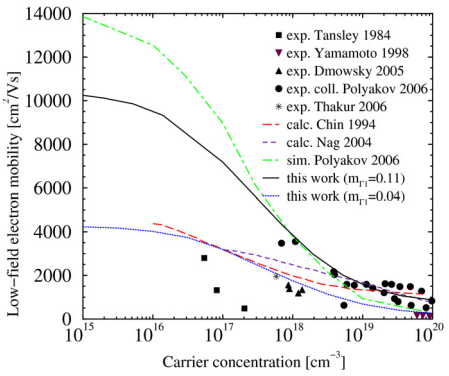

Fig. 1: Low-field electron mobility as a function of carrier concentration in InN: Comparison of the MC simulation results and experimental data.

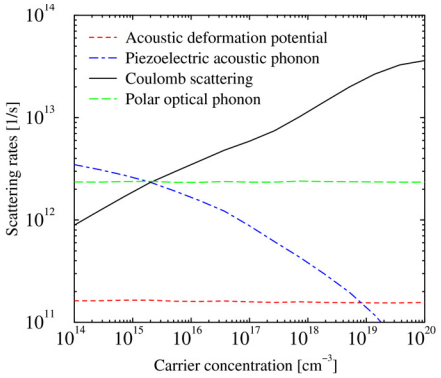

Fig. 2: Illustration of the corresponding scattering rates in the Monte Carlo simulation of mobility as a function of carrier concentration at 300 K

As a particular example, Fig. 1 shows the low-field electron mobility in hexagonal InN as a function of free carrier concentration. Results from other groups [7, 9, 19] and various experiments [19, 20, 21, 22] are also included. Assessing the classical band structure model (E_g=1.89 eV), we achieve electron mobility of ≈4000 cm^2/Vs, which is in a good agreement with the theoretical results of other groups using similar setup [7]. Considering the newly calculated band structure model (E_g=0.69 eV), maximum mobility of ≈10000 cm^2/Vs is achieved. The corresponding scattering rates are illustrated in Fig. 2. The increased mobility can be explained with the lower effective electron mass. Polyakov, et al. [8] calculated a theoretical limit as high as 14000 cm^2/Vs, however their simulation does not account for piezoelectric scattering, which is the dominant mobility limitation factor at low concentrations (see Fig. 2). Fig. 3 shows the electron drift velocity versus the electric field at 10^{17} cm^{-3} carrier concentration. Our MC simulation results differ compared to simulation data from other groups [8, 13, 14, 23] either due to piezoscattering at lower fields or, at high fields, due to the choice of parameters for the permittivity and polar optical phonon energy ($\hbar\omega_{LO}$). Fig. 4 shows our simulation results obtained with $m_{\Gamma 1}=0.04m_0$ and with different values of the permittivity and phonon energy. The values ε_∞=6.7 and ε_s=11.0 proposed in [9] lead to lower electron velocities.

In summary, a study of the transport properties of InN using two different band structures and two different scattering model parameter sets is performed. A significant increase in the electron mobility and drift velocity is observed when using a parameter set, consistent with the recently reported lower bandgap of InN.

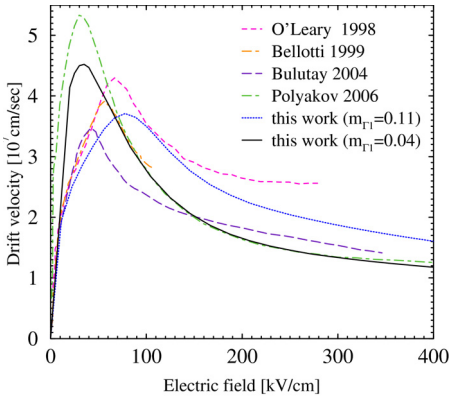

Fig. 3: Drift velocity versus electric field in wurtzite InN: Comparison of MC simulation results.

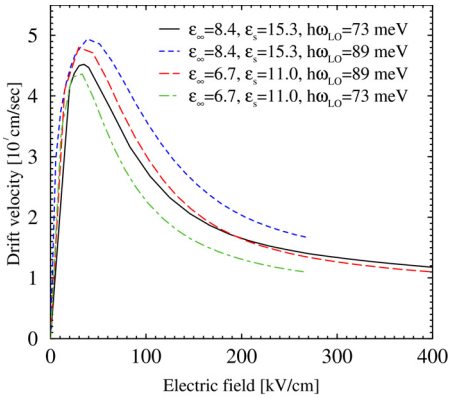

Fig. 4: Drift velocity versus electric field: Comparison of MC simulation results with different parameter setups.

Acknowledgment: The authors acknowledge support from Austrian Science Funds (FWF), Project START Y247-N13.

References

[1] Wu, J. et al., Phys.Rev.B 66, 201403-1-201403-4, 2002.
[2] Davydov, V. et al., Phys.Status Solidi (b) 230, R4-R6, 2002.
[3] Matsuoka, T. et al., Appl.Phys.Lett. 81, 1246-1248, 2002.
[4] Tansley, T. and Foley, C., J.Appl.Phys. 59, 3241-3244, 1986.
[5] Lambrecht, W. and Segall, B., EMIS Datareview Series 11, 151-156, 1994.
[6] Fritsch, D. et al., Phys.Rev.B 69, 165204-1-165204-5, 2004.
[7] Chin, V. et al., J.Appl.Phys. 75, 7365-7372, 1994.
[8] Polyakov, V. and Schwierz, F., J.Appl.Phys. 99, 113705-1-113705-6, 2006.
[9] Nag, B., J.Cryst.Growth 269, 35-40, 2004.
[10] Vitanov, S., Lecture Notes in Comp. Science 4310, Springer, 197-204, 2007.
[11] Wright, A., J.Appl.Phys. 82, 2833-2839, 1997.
[12] Bernardini, F. and Fiorentini, V., Phys.Rev.B 56, 10024-10027, 1997.
[13] O'Leary, S. et al., J.Appl.Phys. 83, 826-829, 1998.
[14] Bellotti, E. et al., J.Appl.Phys. 85, 916-923, 1999.
[15] Sheleg, A. and Sevastenko, V., Neorg.Mat. 15, 1598, 1979.
[16] Kim, K. et al., Phys.Rev.B 53, 16310-16326, 1996.
[17] Wang, S. and Ye, H., Phys.Status Solidi (b) 240, 45-54, 2003.
[18] Zoroddu, A. et al., Phys.Rev.B 64, 045208-1-045208-6, 2001.
[19] Polyakov, V and Schwierz, F., Appl.Phys.Lett. 88, 032101-1-032101-3, 2006.
[20] Tansley, T. and Foley, C., Electron.Lett. 20, 1066-1068, 1984.
[21] Yamamoto, A. et al., J.Cryst.Growth 189/190, 461-465, 1998.
[22] Dmowski, L. et al., Appl.Phys.Lett. 86, 262105-1-262105-3, 2005.
[23] Bulutay, C. and Ridley, K., Supperlatt. and Microstructures 36, 465-471, 2004.